RESEARCH PAPER

EXPLORING THE POTENTIAL OF 6-BROMO-2-CHLORO-QUINOLINE SCHIFF BASES TARGETING ANGIOGENESIS FOR CANCER: SYNTHESIS, IN-SILICO AND IN-VITRO STUDY

Mounika Tummalapalli[1], Ravi Sankara Reddy Dontireddy[2]*

[1]Research Scholar, Department of Pharmaceutical Chemistry, University College of Pharmaceutical Sciences, Acharya Nagarjuna University, Nagarjuna Nagar, Guntur-522510, India.

[2] Assistant Professor, Department of Pharmaceutical Chemistry, University College of Pharmaceutical Sciences, Acharya Nagarjuna University, Guntur-522510, India.

*E-mail: drsrpharma@gmail.com

*Corresponding Author: Ravi Sankara Reddy Dontireddy**

ABSTRACT

In the present scenario, cancer remains a major therapeutic challenge due to its aggressive nature. Currently, cancer research targeting the pathways responsible for pathogenesis, among many angiogenesis plays a vital role in tumor growth and metastasis. VEGFR, EGFR and MMP-9 are key regulators of angiogenesis, tumour proliferation and metastasis, representing potential multi-target therapy. Quinoline-based Schiff bases have demonstrated promising anti-cancer potential. The study aimed to design, synthesis and evaluate a new series of 6-bromo-2-chloro quinoline Schiff bases (S3F3-S3J8) as multi-targeted anti-cancer agents. The target compounds were synthesised by condensation of 6-bromo-2-chloro quinoline-3-carbaldehyde with substituted hydrazine and aryl amines using traditional stirring and microwave irradiation respectively. All the title compounds structurally confirmed using IR, NMR and Mass spectroscopic analysis. Cytotoxicity was evaluated by MTT assay against MDA-MB-231 cell line and selectivity index was calculated. Along with this, anti-metastatic activity was confirmed by gelatin-zymography for MMP-9 inhibition. Molecular docking was performed using AutoDock 4.1.2 against VEGFR (4ase), EGFR (7aei) and MMP-9 (5i12) and atomic interactions were visualized in Discovery studio. Compound S3F3 exhibited the most potent cytotoxic activity against Breast cancer cell lines with an IC_{50} value of 100.34µM. Based on selectivity index, S3F3 displayed 2.3 folds more cytotoxicity compared to normal cell. Gelatin zymography revealed significant inhibition of MMP-9 (40%) compared to standard diclofenac. Docking analysis showed strong binding affinity of S3F3 (-11.28, -9.32 and -14.15 kcal/mol) against VEGFR2, EGFR and MMP-9 respectively with favourable hydrogen bond and hydrophobic interactions within the binding pocket. The findings suggest that compound S3F3 can serve as a promising lead for the development of multi-targeted agents against breast cancer. Further *in-vivo* and mechanistic studies are required to establish complete preclinical data.

Keywords: 6-bromo-2-chloroquinoline-schiff bases, angiogenesis, gelatin zymography, VEGFR2, molecular docking, anti-cancer activity.

How to cite this article: Mounika Tummalapalli1 Ravi Sankara Reddy Dontireddy2*. EXPLORING THE POTENTIAL OF 6-BROMO-2-CHLORO-QUINOLINE SCHIFF BASES TARGETING ANGIOGENESIS FOR CANCER: SYNTHESIS, IN-SILICO AND IN-VITRO STUDY. Int J Drug Deliv Technol. 2026;16(90s):2042-2055. DOI: 10.25258/ijddt.16.90s.204.

INTRODUCTION

Globally, cancer incidence was slightly increased in women particularly breast cancer while colorectal, lung cancers in men. According to American Cancer Society, roughly 20 million new cases and nearly 10 million deaths were reported each year. According to WHO, annual new cancer cases are projected to be double by 2050 due to population growth and aging [1]. Angiogenesis plays a pivotal role in tumor growth and metastasis to meet the tumor cell oxygen and nutrient requirement. It is the chemical driven physiological process of formation of new blood vessels from pre-existing vasculature through endothelial cells [1, 2]. It is primarily regulated by feedback mechanism of proangiogenic and anti-angiogenic factors, balances the activation and inactivation of angiogenesis [3]. The proangiogenic factors like VEGF/VEGFR, PDGF-B, Notch, FGF-2, IL-8, TNF-α, TNF-β were released during cell development, regeneration, hypoxia and inflammation. Endostatins, constatin, tumstatin, angiostatin, thrombospondins are released in normal cells to block angiogenesis. But in tumor cells, anti-angiogenic pathway gets supressed and proangiogenic pathway is stimulated. Among all the pathways, VEGF/VEGFR pathway is most significant in promoting angiogenesis. There are 5 types of VEGFs and 3 types of VEGFR. [3,4] Only VEGF-A involves in the tumor pathogenesis and it acts on VEGFR-1 and VEGFR-2. VEGFR located on surface of endothelial cells. Angiogenesis starts with the release of VEGF-A from tumor cells by activation of HIF-1α due to the tumor cell hypoxia. Increased VEGF-A in blood, binds to the VEGFR receptors on surface of endothelial cells. VEGF-A has more affinity towards the VEGFR-1 compared to VEGFR-2, but the effect produced by the binding to VEGFR-2 is double than that of the VEGFR-1 [3]. when the VEGF-A binds to the VEGFR-2 receptor,

it undergoes dimerization causes activation of Tyrosine kinase domain leads to autophosphorylation of tyrosine residue in VEGFR-2. Lipases (PLCγ) and kinases (PI3K, SrCK) get activated by autophosphorylation thereby activates the gene expression of MMP-9 [4]. When comes to PLC γ activation, PIP3 concerted into IP3, DAG which in turn releases calcium ions, activation of PKC, RAF, MEK, ERK whereas PI3K activates Akt which releases eNOS (endothelial Nitric Oxide Synthase). Combinely, ERK and eNOS, SrcK activates transcription factors like AP-1 and NF-kB. These factors bind to MMP-9 promotor site for enhancing MMP-9 expression. It leads to synthesis of MMP-9 by activation of pro-MMP-9 zymogen and secreted into the extracellular space, which degrades the extracellular matrix [4,5]. Thereby migrating the endothelial cells for blood vessel formation. So, angiogenesis inhibition is achieved by inhibiting any of the step during the angiogenesis process [6].

Targeting angiogenesis offers a broader therapeutic window that many other cancer pathways because it exploits a physiological dependency rather than a tumor-specific mutation [7]. Unlike oncogenes or signalling pathways that vary wildly between patients and develop resistance through single mutations, [8] solid tumors universally require sustained VEGF-A/VEGFR-2 driven angiogenesis to grow beyond 1-2mm and meta size [7,9]. Normal adult vasculature is quiescent with endothelial turnover measured in years and low VEGF dependence. [10] So, anti-angiogenic drugs preferentially collapse the immature, pericyte poor, VEGF addicted tumor vessels [11]. This quiescence versus activation difference creates selectivity without needing a tumor-specific antigen, providing activity across diverse histologies [9, 12]. Moreover, endothelial cells are genetically stable diploid cells, making them less prone to drug-resistance mutations than genetically unstable tumor cells [8] and pruning chaotic tumor vasculature can transiently normalize blood flow to improve delivery of chemotherapy and immune cells [11]. Thus, despite on target toxicities and kidney function [13,14] angiogenesis inhibition provides relatively, tumor-selective, histology-agnostic pressure than blocking a single mutated kinase [8, 9].

Since decades, intense research is going on focusing VEGFR/VEGF signalling pathway to develop anti-cancer agents which inhibit angiogenesis. USFDA approved drugs as VEGFR-2 antagonists acts on different cancers with key pharmacophoric features (Figure 1). VEGFR-2 inhibitors observed in FDA approved drugs from published literature was found to be a hetero aromatic ring structure capable of engaging Cys917 at the hinge region [15,16], A spacer moiety capable to be directed in the spacer region of the active site, a pharmacophore moiety (e.g. amide or urea) that can bind to Glu883 and Asp1044 at the DFG motif region, a hydrophobic group resides in the allosteric pocket of the VEGFR-2 binding site [15,16]. Carbozantinib **1** a multi-kinase inhibitor with IC50 values of 0.035nM, Foretinib **2** used as multitarget inhibitors in treatment of Lung, Ovarian, Gastric cancer with IC50 0.9nM, Lucitanib **3** a multitarget inhibitor of solid tumors with IC50 25nM, Lenvatinib **4** used in treatment of renal, hepatic cancers with IC50 4nM, Tivozanib **5** another anti-cancer drug targeting selectively to VEGFR2 and used in renal cancer with IC50 0.16nM [15]. Over the last decade, substantial work reporting on quinoline ring potential as VEGFR2 inhibitors. The study by Elkaeed, reported that quinoline coupled with thiazodione aryl amide **6,7** displayed good anti-proliferatory activity by inhibiting VEGFR2 receptors (IC50 137.40, 98.53nM) and against MDA-MB231 breast cancer cell lines (125.5, 188µM) [15]. Hussein works on anti-proliferative activity of aryl substituted isoserine linked triazole-quinoline derivatives **8** against MCF7 breast cancer cell lines (IC50 112.31µM) [17], Lix designed and evaluate the 3-aryl quinoline derivatives as anticancer agents tested in MCF7 cancer cell lines, targeting VEGFR-2 (IC50 1.8 µM) [18]. Taghour Mohammed designed thiazolidine-2,4-dione hybrid with 1,2-dihydroquinolones **10, 11** [19] against VEGFR2 (IC50 96.64, 317.7nM) and breast cancer cell lines (IC50 150, 70 µM) (Figure 2). Based on the key features of VEGFR2 antagonists with quinoline ring including the previously published moieties, molecular hybrids were designed with slight modification in the hydrogen bond acceptors and donors (urea and amide replaced with Schiff bases) and in terminal aryl ring with fused heterocycle coumarin.

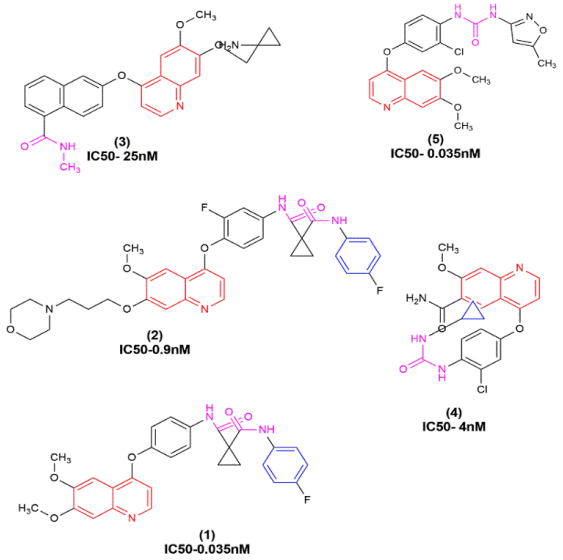


Figure 1: USFDA approved quinoline ring containing VEGFR2 antagonists

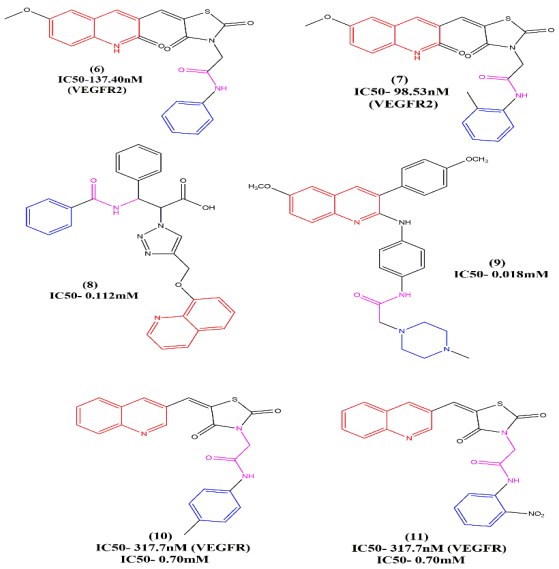


Figure 2: Reported quinoline derivatives as anti-proliferative drugs

MATERIALS AND METHODS

Materials:

All the chemicals purchased from Otto Scientific Chemicals, TCI chemicals and Merc Sigma Aldrich were used without purification. Bruker FTIR, 400MHz, 100MHz NMR spectrometer used to analyse IR, proton, carbon spectra. ESI-MS, MS +Q centroid spectrum used to analyse mass spectral data of synthesised compound. Gallen Hemp Melting Point Apparatus used to identify melting point. Precoated aluminium plates were used for thin layer Chromatography. TLC was checked throughout the synthesis to identify product formation.

Chemistry:

Scheme 1a- Synthesis of 6-bromo-2-chloro quinoline-3-carbaldehyde: In the first step, 4-bromo acetanilide **B** prepared from 0.06mol of acetanilide **A** (8.11g) in 40ml glacial acetic acid (GAA), 0.06mol bromine solution (3.12 ml in 10ml GAA) added dropwise under cool bath for 15min. with continuous stirring until product formation. the solid precipitate was then filtered using normal filter paper and washed thoroughly with ice water to remove excess GAA. Dried and recrystalized the product using ethanol. Then mix POCl3 (0.5mol, 47ml) dropwise to the ice cold DMF (0.15mol, 12ml) with continuous stirring. And reflux the mixture at 80-90^{0}C after addition of 4-bromo acetanilide **B** (0.05mol, 10.5g) for 7hrs. Then cool the reaction mixture to room temperature and solid precipitate was formed immediately by adding reaction mixture into cold water. The product 6-bromo-2-chloro quinoline-3-carbaldehyde **C** was dried and recrystallized with ethyl acetate [20].

Scheme 1b- Synthesis of 3-ethanehydrazonoyl chromen-2-one: Equimolar concentration of salicylaldehyde **D** (0.1mol, 12.2ml), ethyl acetoacetate (0.1mol, 13.01ml) and catalytic amount of piperidine under stirring at room temperature for 20 hrs. Scrape and collect the product, neutralize the piperidine with 200ml of 0.1M HCl solution. Filter the solid, wash with distilled water and recrystallized the 3-acetyl coumarin **F** with ethanol [21]. With the modification of Parquet E procedure [22] 3-ethanehydrazonoyl chromen-2-one was prepared. Mix the equimolar concentration of 3-acetyl coumarin **E** (10mmol), hydrazine hydrate (10mmol) and 10ml of ethanol solvent in reaction vessel. Add few drops of GAA for maintaining acidic pH, reflux under microwave irradiation at 400W power for 2 min. Cool the mixture and transfer to beaker containing ice cold water to get precipitate. Filter the solution under suction and recrystallize the 3-ethanehydrazonoyl chromen-2-one **F** with ethanol.

Scheme 1c- Synthesis of title compounds S3F3, S3H3, S3J6-S3J8: Equimolar concentration (7mmol) of 6-bromo-2-chloroquinoline-3-carbaldehyde **E**, 3-ethanehydrazonoyl chromen-2-one **F** and 10ml of ethanol under stirring at room temperature with 500-700 rpm for 3hrs. add cool water into the mixture and filter under suction. Dry the product after washing with cold water and recrystalize the solid product with ethanol.

General Procedure for synthesis of S3H3 and S3J6-S3J9: Equimolar concentration of 6-bromo-2-chloro quinoline-3-carbaldehyde and phenyl hydrazine, substituted aryl amines (o-phenylene diamine **I1**, 4-aminno acetanilide **I2**, 4-amino carboxylic acid **I3**) in 10ml of ethanol and catalytic amount of GAA (3 drops) under microwave irradiation at 300W for 3-4 min. the mixture were cooled to room temperature and add cool water to get precipitate, filter and dried the product [22]. Recrystallized with ethanol.

4-bromoacetanilide (B): white crystals, yield: 83.6%, M.P.: 162-163^{0}C; H^1 NMR (400MHz, dmso, ppm): 10.61 (s, 1H, Amide NH), 7.452-7.563 (m, 4H, Ph-CH), 2.039 (s, 3H, Acetyl CH). C^{13} NMR (100MHz, dmso, ppm): 168.47 (s, 1C, Amide CO), 138.68 (Ph-C1-NHCO, s, 1C), 131.454, 128.630 (meta carbons, s, 2C)120.85, 118.966 (ortho Carbons, s, 2C), 114.49 (Br-C4-Ph, s, 1C), 24.021 (Acetyl CH, s, 3C); Mol. Formulae: C_8H_8ONBr; Mol. Wt.: 214.06 (calculated); Mass (m/z): 213.99 [M+H], 215.99 [M+2], 236.02 [M+Na], 251.93 [M+K], 158.10 (Base peak).

6-bromo-2-chloro quinoline-3-carbaldehyde (C): Yellow solid, yield: 79.5 %, M.P.: 136-138^{0}C ; H^1 NMR (400MHz, dmso, ppm): 10.372 (s, 1H, CHO), 8.962 (s, 1H, C4), 8.603-8.597 (d, 1H, C5), 8.12-8.093 (dd, 1H, C8), 7.99-7.97 (d, 1H, C7); C^{13} NMR (100MHz, dmso, ppm): 189.16 (s, 1C, CHO), 149.59 (s,1C, C8a), 147.145 (s, 1C, C2), 140.305 (s, 1C, C3), 136.608 (s, 1C, C4a), 131.962 (s,1C, C4), 129.875 (s, 1C, C8), 127.658 (s,1C, C5), 127.028 (s,1C, C7), 121.107 (s,1H, C6); Molecular Formulae: $C_{10}H_5ONClBr$; Mol. Wt.: 268.92 (cal); Mass (ESI, m/z): 271.45 [M-H]$^-$, 272.11 [M+2], 158.82 (base peak).

3-acetyl coumarin (E): Pale yellow crystals, yield: 85.10%; M.P.:120-122^{0}C; IR (KBr cm^{-1}): 3090 (Ar CH, str), 2910 (Methyl CH, str), 1746.32 (lactone C=O, str), 1718.90 (Acetyl C=O, str),1459.81 (Ar C=C, str), 1040 (coumarin C-O-C, str); H^1 NMR (400MHz, CDCl3, ppm): 8.517 (s, 1H, C4), 7.681-7.64 (m, 2H, C6, C7), 7.394-7.33 (dd, 2H, C5, C8), 2.735 (s, 3H, methyl CH); C^{13} NMR (400MHz, CDCl3, ppm): 195.213 (s, 1C, acetyl Carbon), 158.987 (s, 1C, C2), 155.092 (s, 1C, C8a) 147.235 (s, 1C, C4); 134.231 (s, 1C, C3), 130.086, 124.810, 124.302, 118.054 (4C, C5, C6, C7, C8), 116.452 (1C, C4a), 30.343 (s, 1C, methyl C); Molecular Formulae: $C_{11}H_8O_3$; Molecular weight: 188.18 (calculated); Mass (ESI, m/z):189.07 [M+H].

3-ethanehydrazonoyl chromen-2-one (F): Pale yellow solid, Yield 72.4%, M.P.: 196-197^{0}C; IR (KBr, cm^{-1}): 3430 (hydrazone NH, str.), 3100 (hydrazone CH, str.), 3059 (Ar CH, str.), 2960 (Methyl CH, str.), 1778.81 (Lactone C=O, str.), 1660.52 (Hydrazone C=N, str.), 1460.79 (Ar C=C, str.), 1034.80 (Coumarin C-O-C, str.), 1000.59 (Hydrazone N-N, str.); H^1 NMR (400MHz, dmso, ppm): 11.218, 11.133 (s, 2H, Hydrazone NH), 9.009 (s, 1H, hydrazone CH), 8.668 (s, 1H, C4-H), 7.482-7.422 (m, 2H, C5-H, C8-H), 7.708-7.774 (m, 2H, C6-H, C7-H), 2.591 (s, 3H, acetyl CH); C^{13} NMR (100MHz, dmso, ppm): 158.78 (s, 1C, lactone C2), 153.9 (s, 1C, hydrazone N=C-), 155.68 (s, 1C, C8), 153.92 (s,1C, C3),147.153 (s, 1C, C4), 130.84-118.18 (3C, C5, C6, C7), 10.628 (s, 1C, methyl); Mol. Formulae: $C_{11}H_{11}O_2N_2$; Mol. wt.: 202.21; Mass (ESI, m/z): 200.87[M-H].

3-((E)-1-((E)-((6-bromo-2-chloroquinolin-3-yl)methylene)hydrazono)ethyl)-2H-chromen-2-one (S3F3): solid, Yield: 44.38%; M.P.: 112-114^{0}C; IR (KBr cm^{-1}): 3110 (Ar CH, str.), 3010 (hydrazone CH, str.), 2985 (methyl CH, str), 1759.19 (Lactone C=O, str), 1660.30 (Hydrazone C=N, str), 1457.14 (Ar C=C, str), 1314.76 (Quinoline C-N, str), 1014.31 (Hydrazone N-N, str), 767.70 (Ar C-Cl, str), 649.41 (Ar C-Br); H^1 NMR (400MHz, dmso, ppm): 10.374 (s, 1H, azine -CH=N-N=C-), 8.670 (s, 1H, C4^1-H $_{Quin}$), 8.612-8.607 (d, 1H, C4-H Coumarin), 8.099-8.104 (d, 1H, C8^1-H $_{Quin}$), 7.955 (s, 1H, C7^1-H $_{Quin}$), 7.934 (s, 1H, C5^1-H Quin), 7.772-7.736 (t, 2H, C6-H, C7-H Coumarin), 7.484-7.36 (m, 2H, C5-H, C8-H Coumarin), 2.590 (s, 3H, Methyl CH); C^{13} NMR (100MHz, dmso, ppm): 158.403 (s, 1C, lactone C=O), 154.57 (s, 2C, Azine -C=N-N=C-), 150.011 (s, 1C, C2^1 $_{Quin}$), 147.016 (s, 2C, C8 & C8^1 $_{Quin}$), 136.58 (s, 1C, C4^1), 134.45 (s, 2C, C4 & C7^1), 130.748 (s, 2C, C7 & C5^1), 129.867 (s, 1C, C8^1), 127.9 (s, 1C, C3^1), 127.57 (s, 1C, C5^1), 124.91 (s, 1C, C6), 124.409 (s, 1C, C4a^1), 121.19 (s, 1C, C6^1), 118.131 (s, 2C, C4a & C8), 116.082 (s, 1C, C3); Molecular Formulae: $C_{21}H_{13}O_2N_3ClBr$; Molecular weight: 456.73(calculated); Mass (ESI, m/z): 455.68[M+H], 457.54[M+2], 458.74[M+4], 114[base peak].

6-bromo-2-chloro-3-((2-phenylhydrazono)methyl)quinoline (S3H3): solid, Yield: 44.29%; M.P.: 156-158^{0}C; IR (KBr cm^{-1}): 3250 (Hydrazone NH, str.), 3097 (Ar CH, str.), 3008 (Hydrazone CH, str.), 1650.05 (hydrazone C=N, str.), 1456.39 (Ar C=C, str.), 1319.13 (Quinoline C-N, str.), 753.30 (Ar C-Cl, str.), 636.92 (Ar C-Br, str.); H^1 NMR (400MHz, dmso, ppm): 11.071 (s, 1H, -HC=N-N-), 10.37 (s, 1H, -C=N-NH), 8.921 (s, 1H, C4-H), 8.462 (s, 1H, C5-H), 8.227 (s, 1H, C8-H), 7.869 (s, 1H, C7-H), 7.306-7.251 (dd, 2H, C2^1-H & C6^1-H), 7.204-7.185 (C5^1-H & C3^1-H), 6.889-6.833 (t, 1H, C4^1-H); C^{13} NMR (100MHz, dmso, ppm): 148.35 (s, 1C, C2), 147.123 (s, 1C, C8a), 144.52(s,1C, -C=N-NH), 144.44 (s, 1C, C4^1), 140.218 (s, 1C, C3), 136.552 (s, 1C, C4a), 131.93(s, 1C, C4), 129.973 (s, 1C, C8), 129.829 (s, 1C, C3^1), 129.68 (s, 1C, C5^1), 128.62 (s, 1C, C5), 127.635 (s, 1C, C7), 121.071 (s, 1C, C6), 120.464 (s, 1C, C2^1), 119.89 (s, 1C, C6^1); Molecular Formulae: $C_{16}H_{11}N_3Cl$ Br; Molecular weight: 360.64 (calculated); Mass (ESI, m/z): 360.10[M+H], 362.01[M+2], 364.06[M+4], 114.98 [base peak].

N1-((6-bromo-2-chloroquinolin-3-yl)methylene)benzene-1,2-diamine (S3J6): solid, Yield: 65%; M.P.; 131-132^{0}C; IR (KBr cm^{-1}): 3349.76 (NH_2 str), 3043.29 (Ar-CH str), 1632.01 (-CH=N- str), 1574.95 (C=N str), 1468.89 (Ar-C=C str), 1286.46 (Ar-C-N str), 735.47 (Ar-Cl str), 677.62 (Ar-Br, str); H^1 NMR (400MHz, dmso, ppm): 8.492 (d, 1H, C4), 8.038 (s, 1H, -CH=N-), 7.738-7.631 (m, 3H, Quin CH), 7.421 (s,1H, Phenyl C3^1-H), 6.563-6.674 (d, 3H, Phenyl CH), 5.862 (s, 2H, Ar-NH); C^{13} NMR (100MHz, dmso, ppm): 168.00 (s, 1C, Quin C2), 153.60 (s, 1C, -CH=N-), 131.70 (s, 3C, Quin C5, C7, C8), 117.38 (s, 1H, Quin C3), 113.06 (s, 3C, Ph C3, C4, C5), 112.39 (s, 1C, Ph C6), low intensity peaks without proper detection (120-151ppm, 5C); Molecular Formulae: $C_{16}H_{10}ClBrN_2$; Molecular weight: 358.98 (calculated); Mass (ESI, m/z): 399.01([M+K] adduct due to traces of K^+), 400.98 [M+K+2], 402.95 [M+K+4](isotopic abundance of halogens in 3:4:1 intensity), 388.93 (Base peak).

N-(4-(((6-bromo-2-chloroquinolin-3-yl)methylene)amino)phenyl)acetamide (S3J7): solid, Yield: 70.8%; M.P.:134-135^{0}C; IR (KBr cm^{-1}): 3254.44 (Ar-NH-CO-, str), 3080.09 (Ar-CH, str), 2924.92 (methyl CH, str), 1690 (amide C=O, str, very week), 1662.99 (imine C=N, str), 1592.13 (C=N), 1520.26 (Ar C=C, str), 1345.95 (Ar C-N), 816.21 (Ar Cl, str), 693.33 (Ar Br, str); H^1 NMR (400MHz, dmso, ppm): 10.144 (t, 1H, amide NH), 9.62 (s, 1H, imine CH), 8.912 (d, 1H, C4$_{quin}$), 8.502 (s, 1H, C5 $_{quin}$), 8.283-80215 (d, 1H, C8$_{quin}$), 7.955 (s, 1H, C7$_{quin}$), 7.507-7.116 (m, 4H, phenyl CH), 2.018 (s, 3H, methyl CH); C^{13} NMR (100MHz, dmso, ppm): 168.97 (s, 1C, amide CO), 168.02 (s, 1C, C2$_{quin}$), 150.43 (s, 1C, Imine C=N), 146.66-121.24 (s, 9C, quinoline), 120.58 (s, 1C, C4

phenyl),115.56-120.19 (s, 4C, phenyl ortho and meta carbons), 118.72 (s, 1c, C1 phenyl); Molecular Formulae: $C_{18}H_{13}ON_3ClBr$; Molecular weight: 401.99 (calculated); Mass (ESI, m/z): 402.04 [M+H], 404.03 [M+2], 406.03 [M+4], 457.98 (Base peak).

4-(((6-bromo-2-chloroquinolin-3-yl)methylene)amino)benzoic acid (S3J8): solid, Yield: 73.38%; M.P.:138-140^{0}C; IR (KBr cm^{-1}): 3334.43 (C-OH, str), 3101.05 (Ar C-H, str), 1827.92 (C=O, str), 1675.75 (imine C=N, str), 1592.99 (C=N, str), 1420.27 (Ar C=C), 1280.89 (Ar C-N, str), 1164.75 (C-O, str), 764.44 (Ar Cl, str), 694.73 (Ar Br, str); Molecular Formulae: $C_{17}H_{10}O_2N_2ClBr$; Molecular weight: 387.962 (calculated); Mass (ESI, m/z): 388.99 [M+H], 390.99 [M+2], 393.00 [M+4], 457.98 (base peak).

***In-silico* studies**

Molecular Docking studies: Molecular docking was performed using AUTODOCK. All the ligand structures were drawn using Chemdraw ultra12.0 and minimized the energies using chem3D pro of chem biooffice suite. Macromolecules like VEGFR2, EGFR receptor and MMP9 structures were retrieved from protein data bank [23-28] database (pdbid- 4ASE, 7AEI & 5I12) of resolution 1.83, 2.65 & 1.59A^0 complexed with tivozanib, base plate protein and aryl sulfonamide carboxylate respectively. Protein cleaning by removal of water, non-standard molecules like inbuild ligands and small molecules followed by addition of kollmann charges and polar hydrogens. Grid box was generated (x, y, z 40, 40, 40A^0) by locating the active pocket of the macromolecules using prank web database. And docking was run using command prompt with grid and dock parameter files. Finally, best confirmation was saved and analyse the atomic interactions using discovery studio visualizer.

***In-vitro* studies**

Cell viability assay: The cytotoxicity potential of the test compounds was performed using the 3-(4,5-dimethylthiazol-2yl)-2,5-diphenyltetrazoliuum bromide (MTT) assay with minor modifications in Hattiholi procedure [29]. MDA-MB-231 human breast adenocarcinoma cells (NCCS, Pune), L929 mouse-derived fibroblast cell lines (NCCS, Pune) were cultured in Dulbecco's modified Eagle Medium (DMEM, low glucose, Thermo fisher scientific, cat.no. 11885-084) supplemented with 10% fetal bovine serum (FBS, Hi Media, Mumbai, Cat. No. RM10409) and 1% anti-biotic-antimycotic solution (Thermo Fisher Scientific, Cat. No. 15240062). Cells were maintained at 37^{0}C in a humidified atmosphere of 5% CO_2. For the assay, cells were seeded at a density of 1x10^4 cells/well in 96-well flat-bottomed microplates and allowed to adhere overnight. The cells were then treated with varying concentrations of the test samples (100, 50, 25, 12.5, 6.25, 3.12µg/ml) and incubated for 48hrs. Untreated cells in complete medium served as the negative control. Following treatment, cells were washed twice with phosphate-buffered saline (PBS) and 20µL of MTT solution (5mg/ml in PBS, Thermo Fisher Scientific, Cat. No. M5655-100MG) was added to each well. After 4hrs of incubation at 37^{0}C, the formazan crystals formed by metabolically active cells were solubilized with 100µL of dimethyl sulfoxide (DMSO). Absorbance was measured at 570nm using a microplate reader. Cell viability was expressed as a percentage relative to the untreated control. Selectivity index was calculated using IC50 values of both normal cell lines and cancer cell lines using the formulae [30].

$$Selectivity\ Index\ (SI) = \frac{(IC50\ against\ L929cells)}{(IC50\ against\ MDA-MB-231cells)}$$

Gelatin zymography Assay: MMP-9 activity was assessed by gelatin zymography with minor modifications to the Souza and Patricia procedure [31-32]. Resolving gels (10%) containing 1 mg/mL gelatin were prepared and overlaid with a 4% stacking gel. Tissue samples were collected from squamous cell carcinoma of buccal mucosa, minced in extraction buffer, stored at -20°C, thawed and centrifuged at 3000 rpm for 10-15 min and the supernatant was used for analysis. Test compounds were prepared at 50 mg/mL in DMSO and pre-incubated with 50 µL of sample supernatant for 1 h at room temperature. A negative control containing only sample supernatant and a positive control containing sample with diclofenac sodium (20 mg/mL) were included. Following incubation, samples were mixed with an equal volume of 2X non-reducing sample buffer and 25 µL was loaded per well. Electrophoresis was performed at 80 V until the bromophenol blue dye front reached the bottom of the gel. After electrophoresis, gels were washed for 1 h in 2.5% Triton X-100 to remove SDS and then incubated overnight at 37°C in zymogram incubation buffer. Gels were stained with 0.1% Coomassie Brilliant Blue R-250 for 1 h and destained until clear proteolytic bands appeared against a blue background. MMP-9 (gelatinase-B, ~95 kDa) and MMP-2 (gelatinase-A, ~72 kDa) were identified by their molecular weights. Gel images were captured using a gel documentation system and band intensities were quantified using *Total Lab* software. DMSO served as the vehicle control and diclofenac sodium as a positive control (Inhibitor).

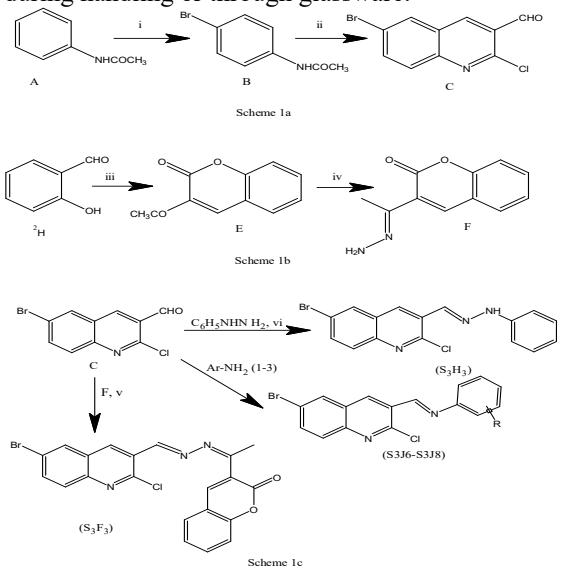
RESULTS AND DISCUSSION

Chemistry

Title compounds 6-bromo-2-chloro quinoline Schiff bases were prepared by multistep synthesis using conventional stirring and moderate microwave irradiation. In the first step, acetanilide **A** undergoes bromination with bromine in glacial acetic acid maintaining cool temperature yields p-bromo acetanilide **B** (scheme 1a) followed by vilsmeier Hack cyclization and formylation with vilsmeier

reagent (POCl3 with DMF) in 1:9:4 ratio under reflux at 90-100^{0}C, get the intermediate 6-bromo-2-chloro-quinoline-3-carbaldehyde **C** (scheme 1a). In the next step, salicylaldehyde **D** undergoes Knoevenagel condensation with ethyl acetoacetate in presence of basic medium facilitated by pyridine as catalyst yields 3-acetylcoumarin **E** by lactonization nothing but intramolecular cyclization (scheme 1b). Then 3-acetyl coumarin reacts with hydrazine in presence of GAA to provide acidic medium for formation of carbonium ion and ethanol stabilizes it and favours nucleophilic attack of hydrazine for formation of the coumarin-hydrazone **F** intermediate under microwave irradiation at power level 3 (300W) scheme 1b. In the next scheme 1c, 6-bromo-2-chloro quinoline-3-carbaldehyde **C** undergoes condensation reaction with coumarin hydrazone **F** in presence of ethanol and GAA by stirring for 4hrs at room temperature forms quinoline-coumarin azine **S3F3**. Phenyl hydrazine **G** and substituted aryl amines **I1-3** reacts with 6-bromo-2-chloro-quinoline-3-carbaldehyde **C** undergoes condensation in presence of ethanol and slight acidic medium provided by GAA under microwave irradiation at power level 3 for 3-4 min. yield respective hydrazone **S3H3** and imine Schiff bases **S3J6-S3J8** (scheme 1c).

All the intermediates and final compounds were characterized using spectral data for structure confirmation after checking TLC using mobile phase chloroform and ethanol (7:3), Ethyl acetate and chloroform (4:6). The identification of key functional groups present in the compound structure was confirmed based on the IR spectral data by its wavenumber values. The major functional groups like lactone ring, hydrazone, imine, azine, aldehyde, acetyl and amide were interpreted for structural confirmation of intermediates and final compounds by spectral analysis [20]. The IR values were 1746.32- 1778.81 cm^{-1} attributed to Lactone C=O, 1030.92-1040 cm^{-1} attributed to coumarin C-O-C, 1650.05- 1660.52 cm^{-1} hydrazone C=N, 1675.75-1632.01 cm^{-1} attributed to imine C=N, 1574.95-1592.99 cm^{-1} attributed to quinoline C=N, 636.92-694.73 cm^{-1} attributed to aromatic C-Br, 816.21-735.47 cm^{-1} attributed to aromatic C-Cl. The NMR spectral values of key functional groups of synthesized compounds are about 2.039 to 2.735 ppm and 24.021 to 30.343 ppm for acetyl CH_3 protons and carbons, 11.071-9.62 ppm and 154.57-144.52 ppm for Schiff base CH proton and carbon chemical shift, 158.40-158.98 ppm value for lactone carbon, protons and 8.962-8.49 ppm for C4 proton of pyridine ring, 168.02-148.35 ppm for chloro substituted carbon of pyridine ring, 8.668-8.607 ppm for lactone C4 proton, aromatic protons and carbon (phenyl, chromene and quinoline rings) chemical shift values ranges from 6.83-8.603 ppm and 114.49-155.09 ppm respectively. All the spectral values are interpretated based on the general ranges from standard text books [33-35]. Mass spectral data gives the information about molecular mass and the interpretation of synthesized compounds are done by analysing both positive ionization and negative ionization spectral data. Mass fragmentation particularly base peak gives the information about stable fragment, m/z values varying 2 units means M+, M+2, M+4 gives information about presence of 2 halogen atoms due to isotopic abundance. In the spectra of S3J6 there is an observation of potassium adduct fragment (M+K) which may occur due to the traces of alkali salts in solvents or may introduced during handling or through glassware.



Scheme 1: Multistep synthesis of aryl substituted 6-bromo-2-chloro quinoline Schiff bases S3F3-S3J8; i-Br, GAA, 0-5^{0}C; ii- DMF, $POCl_3$, reflux for 8hrs; iii- ethyl acetoacetate, pyridine, stirring for 20hrs; iv- ethanol, hydrazine, GAA, 400W, 2min. v- ethanol, GAA, stirring for 3 hrs.; vi- ethanol, GAA, 300 W, 3min.; vii- ethanol, GAA, 300W, 4min.; S3J6: R-NH_2; S3J7: R- $COCH_3$; S3J8: R- COOH

Docking

The molecular docking studies assess the binding affinity of ligands towards the receptor and was predicted by using the tool AutoDock with cancer targets (VEGFR2, EGFR, MMP-9). The docking results of the title compounds S3F3-S3J8 against VEGFR2 was about -11.28 to -8.97 kcal/mol and the standard drug axitinib was -10.39 kcal/mol. all the five compounds and standard drug shares same type of conventional hydrogen bond, hydrophobic interactions like pi-sigma, pi-pi stacking, pi-sulphur with different amino acids seen in table 1. But there is a common hydrophobic interaction among all the title compounds and axitinib were Val 899 and Ala 866 (Pi-alkyl) at the binding site (Figure 3). The least binding energy of S3F3 and axitinib might be due to the presence of hydrogen bonding with Cys 919. The docking scores of compounds S3F3-S3J8 against EGFR was about -9.32 to -7.55 kcal/mol and standard erlotinib about -6.85 kcal/mol (table 1). All

the compounds share common pi-sigma and pi-alkyl interaction with Leu 718 apart from other pi-sulphur, pi-alkyl, alkyl hydrophobic interaction and carbon hydrogen bond with different amino acids (Figure 4). And the least binding scores indicating strong binding affinity of S3F3 against 7aei (EGFR) may be due to the more hydrophobic interactions including pi-lone pair bond with Met 793 (2.83 A^0). The docking scores of title compounds (S3F3-S3J8) against MMP-9 (5i12) was about -14.15 to -11.35 kcal/mol and the standard drug diclofenac was -6.03 kcal/mol (table 1). The atomic interactions of protein ligand complexes of title compounds share pi-pi stacking and pi-cation bond with His 226, pi-alkyl bond with Val 223 (4.81 – 5.32 A^0), alkyl bond with Leu 222 (3.95 – 4.56 A^0). Among all the ligand protein complex, S3F3-MMP-9 displayed highest binding affinity due to more hydrophobic and ionic interactions like pi-cation, pi-sigma. But there are no common interactions with diclofenac, depicted in Figure 5 may be due to missing structural similarity.

Table 1: Docking scores of title compounds S3F3-S3J8 against cancer targets and its atomic interactions.

Protein	Ligand	Scores (kcal/mol.)	Type of Bond	Distance (A^0)	Interacting atom and amino acid residue
VEGFR 2	S3F3	-11.28	CHB π-DHB π-S π-π π-Si	1.99 2.7 4.96 5.36, 5.49 3.78, 3.60	Cys 919 (NH), O Coumarin Asp 1046 (NH), quinoline Cys 1045 (S), quinoline Phe 918 (Ph), Coumarin Leu 1035 (C, Coumarin), Val 899 (C, quinoline)
	S3H3	-8.97	π-Si π-π	3.71, 3.90 4.70	Val 848, Leu 1035 (C, quinoline) Phe 1047 (Ph), quinoline (Ph)
	S3J6	-9.05	π-Si π-S	3.49 5.43, 5.29	Val 899 (C), quinoline (Ph) Cys 1045 (S), quinoline
	S3J7	-10.10	π-Si π- π	3.8, 3.87 5.02, 5.65, 5.21	Leu 840, 1035 (C & quinoline) Phe 918 (Ph, Quinoline) Phe 1047 (Ph, Ph)
	S3J8	-9.41	π-Si π- π	3.76, 4.0 4.75, 5.18 4.69	Leu 840 (C, Quinoline) Phe 918 (Ph, Quinoline) Phe 1047 (Ph, Ph)
	Std1	-10.39	CHB π-S π-Si	1.98, 1.95, 2.02 5.79 3.59, 3.92	Asn 923 (NH, O), Cys 919 (NH, N), Glu 917 (O,

					NH Bp) Cys 1045 (S, Pyridine) Leu 1035 (Bp), Val 916 (Py)
EGFR	S3F3	-9.32	π-Si π- π	3.86, 3.54 4.49	Leu 718 (C, Coumarin), Val 726 (C, Quinoline) Phe 723 (Ph, Quinoline)
	S3H3	-7.84	Ca HB π-S π-Si	3.30 4.82 3.54	Met 793 (O, C) Cys 775 (S, Ph) Leu 718 (C, Quinoline)
	S3J6	-7.55	π-Si	3.93, 3.81, 3.87 3.56	Leu 718 (C, Quinoline) Leu 844 (C, Ph)
	S3J7	-8.79	π-Si	3.30 3.87, 3.70	Leu 844 (C, Ph) Leu 718 (C, Quinoline)
	S3J8	-8.54	π-Si	3.62, 3.57	Leu 718 (C, Quinoline), Leu 844 (C, Ph)
	Std3	-6.85	CH B Ca HB	2.12, 1.98 1.81, 2.69	Met 793 (NH &
			π-Si	3.86, 3.64	O, NH & N) Lys 745 (O, CH) Leu 718 (C, Ph), 844 (C, Qzl) Leu 844 (C, Quinoline)
MMP9	S3F3	-14.15	Ca HB π-Si π- π	3.42 3.57 3.77, 3.51	Arg 249 (C, Coumarin) Thr 251 (C, Coumarin) His 226 (Ph, Quinoline)
	S3H3	-11.35	Ca HB π- π	3.70 4.02, 3.85	Leu 243 (C, O), Val 223 (C,N) His 226 (Idz, Quinoline)
	S3J6	-11.99	Ca HB π- π	3.52 4.00, 3.68	Leu 243 (C, O) His 226 (Idz, Quinoline)
	S3J7	-11.29	π-DHB Ca HB π- π	3.02 3.65, 3.33 3.87	Arg 249 (NH, Quinoline) Tyr 245, Met 247 (O, C Imine) His 226 (Idz, Ph)

	S3J8	-12.11	Ca HB π- π	3.40, 3.10, 3.66 3.64, 3.98	Arg 249, Met 247 (C, O), Val 223 (C, N) His 226 (Idz, Quinoline)
	Std2	-6.03	CH B Ca HB	1.96, 2.09 3.50	Pro 246 (NH, O) Tyr 248 (C, Ph)

Std1- Axitinib, Std3- Erlotinib, Std2- Diclofenac, Ph- Phenyl, Qzl- Quinazoline, Idz- Imidazole, CHB- Conentional Hydrogen Bond, CaHB- Carbon Hydrogen Bond, π-DHB- Pi Donar Hydrogen Bond, π-Si- Pi Sigma, π-S- Pi Sulphur, Tyr- threonine, Pro- proline, His- Histidine, Arg- arginine, Met- methionine, Val- valine, Tyr- tyrosine, Leu- leucine, Lys- lysine, Cys- cysteine, Phe- phenylalanine, Val- valine, Glu- glutamic acid, Asp- Aspartic acid.

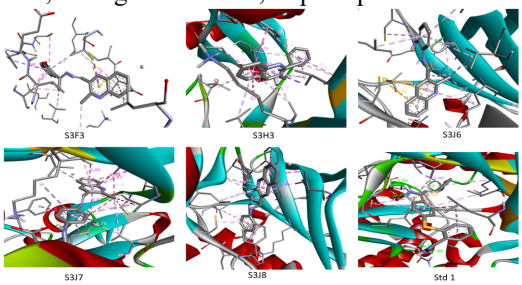


Figure 3: 3d interactions of ligand- protein complex of title compounds and standard drug against VEGFR 2 receptor

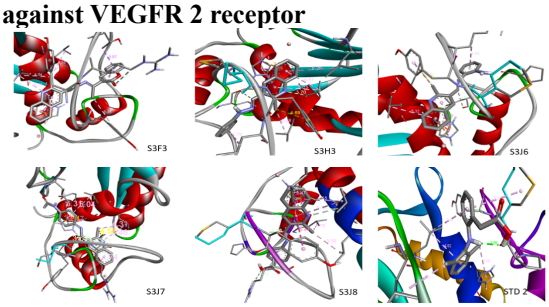


Figure 4: 3d interactions of title compounds and standard drug against MMP9 receptor

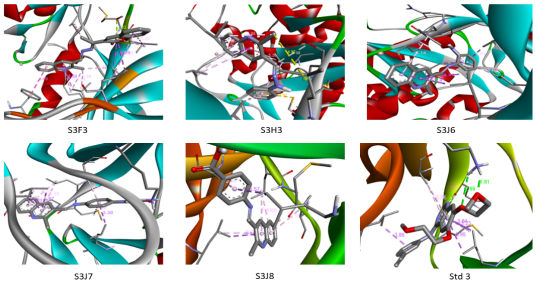


Figure 5: 3d interactions of ligand- protein complex of title compounds, standard drug against EGFR receptor

***In*-vitro Cytotoxicity Assay**

Cell viability percentage of title compounds were assessed against MDA-MB-231 cells using MTT cytotoxicity assay, revealed that all the derivatives displayed moderate to low anti-proliferative activity with IC50 values ranges from 100.34 to 196.46µM presented in table 2. Compound S3F3 exhibited cytotoxicity with 47.03µg/ml (100.34µM), compound S3H3 exhibited cytotoxicity with 55.91µg/ml (155.31µM), compound S3J7 exhibited cytotoxicity with 63.34 µg/ml (155.08 µM), compound S3J6 exhibited cytotoxicity with 70.53 µg/ml (196.46 µM) at 48h. cell viability decreased in a concentration dependent manner from 3.12 to 100 µg/ml (Figure 6). All the test compounds showed cytotoxicity was identified by observing cell morphology including disruption of cell integrity, shrinking and rounding of cells compared to the normal control cells. And there is no significant cytotoxicity was observed in untreated control cells depicted in Figure 7. Data represents Mean ± SD of two independent experiments. Among all the four derivatives, compound S3F3 displayed moderate cytotoxicity (47.03 µg/ml or 100.34 µM) according to NCI guidelines. Among all the title compounds, S3F3 with coumarin ring substitution displayed highest cytotoxicity than the other phenyl hydrazone (S3H3) and substituted phenyl imine derivatives (S3J6-S3J8). It is evident from Mustafa study and Korcz study results [36, 37] on anti-proliferative activity of quinoline-3-carbaldehyde hydrazone derivatives that quinoline ring and pyridine ring substitutions showed more cytotoxicity than the unsubstituted phenyl hydrazone derivative.

The Synthesized compound S3F3 was further evaluated for cytotoxicity against normal L929 fibroblast cell lines. The IC_{50} values were calculated from linear equation (Figure 8) obtained from % of cell viability versus concentration was compared against breast cancer MDA-MB-231 cell lines to determine the selectivity index (SI). S3F3 displayed SI of about 2.283, indicating approximately 2.283 folds greater cytotoxic potency against MDA-MB-231 cell line than the normal L929 cell line. Since, MTT reduction occurs via mitochondrial succinate dehydrogenase, decreased formazan formation indicates loss of mitochondrial metabolic activity. This suggests the compounds induce mitochondrial

dysfunction, though further assays such as Annexin V/PI, ROS or JC-1 are required to confirm apoptosis or necrosis.

Table 2: *In-vitro* cytotoxicity assay of title compounds at different concentrations

Code	Cell viability Percentage (%) against MDA-MB-231 Cell lines						IC50
	100 µg/ml	50 µg/ml	25 µg/ml	12.5 µg/ml	6.25 µg/ml	3.125 µg/ml	
S3F3	14.59 ± 1.65	41.74 ± 6.33	57.86 ± 3.8	69.50 ± 2.79	85.26 ± 5.07	96.91 ± 2.79	47.03
S3H3	21.23 ± 1.39	61.08 ± 6.59	72.10 ± 3.67	68.25 ± 3.04	72.19 ± 3.04	82.85 ± 6.21	55.91
S3J6	42.19 ± 4.93	51.95 ± 4.31	64.94 ± 2.41	70.13 ± 5.45	77.74 ± 5.83	86.61 ± 4.43	70.52
S3J7	32.42 ± 6.59	53.65 ± 5.19	63.41 ± 6.08	75.24 ± 6.08	80.34 ± 4.08	94.76 ± 4.05	62.34
	Cell viability Percentage (%) against L929 Cell Lines						
S3F3	55.93 ± 3.8	77.24 ± 2.4	90.31 ± 1.71	93.22 ± 1.71	103.87 ± 3.08	110.41 ± 0.68	107.36

Duplicate study, values expressed in Mean ± SD

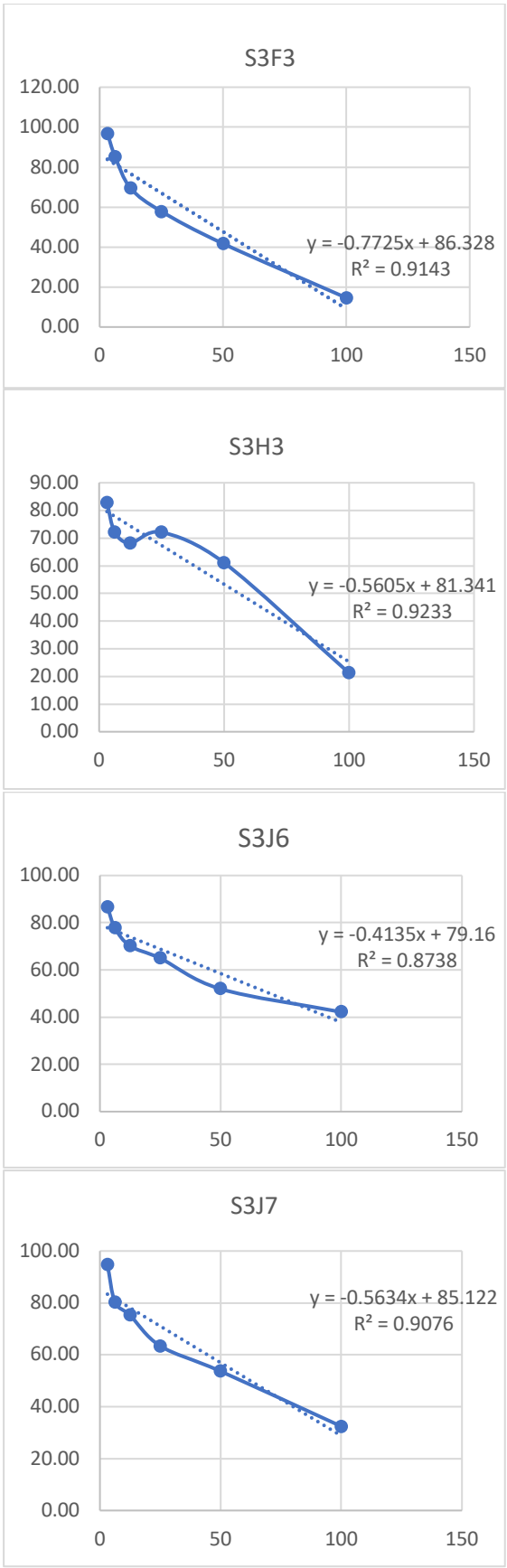
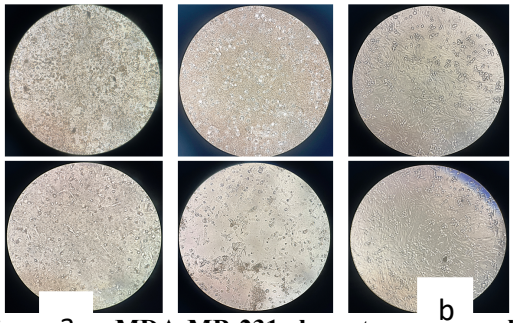


Figure 6: Mean viability (%) Vs Concentration (µg/ml) graph of title compounds against MDA-MB-231 cells



Figur MDA-MB-231 breast ca cells treated with chemicals a-S3F3, b-S3H3, c-S3J7, and d-S3J6 showed morphological changes in light microscopy images. Untreated control cells (e, f) show dense monolayer development and an undamaged membrane. On the other hand, shrinkage, rounding, detachment, decreased cell density, and monolayer disintegration are typical signs of cytotoxicity in treated cells

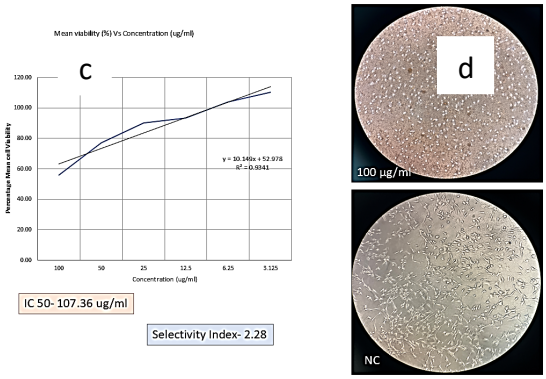


Figure 8: S3F3 cyotoxicity against L929 fibroblast cells and graph of % cell viability versus Concentration; shrinkage, rounding, detachment, decreased cell density and monolayer disintegration observed in treated cells at 100 µg/ml concentration

Gelatin Zymography

Gelatin zymography was performed to evaluate the effect of test compounds on MMP-9 and MMP-2 activity. The assay revealed two distinct lytic bands at approximately 95 kDa and 72 kDa, corresponding to MMP-9 and MMP-2, respectively. The negative control exhibited intense clear bands for both MMP-9 and MMP-2, indicating high gelatinolytic activity. The positive control showed no lytic bands, confirming complete inhibition. Compound in lane 1(S3F3) demonstrated a progressive reduction in band intensity, showing the faintest bands (Figure 9). Notably, displayed the most pronounced reduction in lytic zones, indicating the highest inhibitory potential against MMP-9 and MMP-2. Densitometric analysis revealed that S3F3 inhibited MMP-2 and MMP-9 activity by 63% and 40% respectively, compared to the negative control (table 3). The presence of prominent clear bands in the negative control confirmed active MMP-9 and MMP-2, while their absence in the positive control validated the inhibitory assay. The decreased intensity of lytic zones in lane S3F3 suggests significant inhibition of MMP gelatinolytic activity.

Table 3: Percentage inhibition of MMP-9 and MMP-2 gelatinolytic activity of test compound determined by densitometric analysis of zymograms.

S. No.	Compound Code	Percentage bands of MMP (%)		Percentage inhibition of MMP (%)	
		MMP 2	MMP 9	MMP-2	MMP-9
1.	S3F3	37	60	63	40
2.	NC	100	100	00	00
3.	PC	00	00	100	100

NC: Negative control, PC: Positive control.

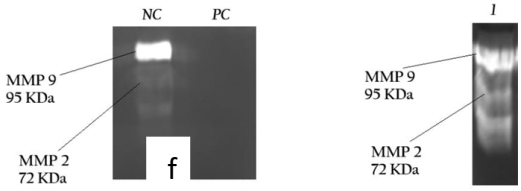


Figure 9: Gelatin zymography showing MMP-9 and MMP-2 activity. NC: Negative control; PC: Positive control. Lane 1: S3F3

CONCLUSION

In the present study, a series of novel 6-bromo-2-chloroquinoline-schiff bases (S3F3-S3J8) were designed, synthesized and structurally characterized. The structures of all synthesized compounds were confirmed by IR, 1H NMR, 13C NMR and Mass Spectroscopy and the spectral data were found to be in good agreement with the proposed structures. All the synthesized compounds were screened for *in-silico* molecular docking studies using AutoDock against 3 targets that is VEGFR2, EGFR, MMP-9 and *in-vitro* cytotoxicity was performed using MTT assay against MDA-MB-231 breast cancer cell lines. Based on these results, the most potent S3F3 compound was further screened for selectivity and metastasis inhibition using Gelatin-zymography assay against MMP-9. The results conclude that S3F3 derivative with coumarin-3-yl substitution displayed 2.3 folds greater cytotoxic activity towards breast cancer cells (IC_{50} 47.03µg/ml) than the normal L929 fibroblast cells (IC_{50} 107.36 µg/ml) and showed moderate MMP-9 inhibition (40%) compared to standard drug diclofenac. Molecular docking results corroborated the *in-vitro* results, showing least binding energies against 3 enzymes might be due to the conventional hydrogen bonding with aminoacids Cys 919 of VEGFR2, hydrophobic interaction with Leu 718 of EGFR and pi-sigma bond with Thr 251 of MMP-9 at their respective binding sites compared to standard drugs. Thus, S3F3 may be considered as a lead molecule for further optimization as a multi-

targeted anti-cancer agent with mechanistic and *in-vivo* studies.

ACKNOWLEDGEMENT

The authors are thankful to the University College of Pharmaceutical Sciences, ANU, Guntur for providing DST-Fist funded laboratory to do this work.

COMPETING INTEREST

Authors declare that, there are no conflicts of interest and the whole work is not funded by any organization.

REFERENCES

1. Liu ZL, Chen HH, Zheng LL, Sun LP, Shi L. Angiogenic signaling pathways and anti-angiogenic therapy for cancer. Signal transduction and targeted therapy. 2023 May 11;8(1):198. DOI: 10.1038/s41392-023-01460-1.
2. Sudan SK, Deshmukh SK, Poosarla T, Holliday NP, Dyess DL, Singh AP, Singh S. Resistin: An inflammatory cytokine with multi-faceted roles in cancer. Biochimica et Biophysica Acta (BBA)-Reviews on Cancer. 2020 Dec 1;1874(2):188419. DOI: 10.1016/j.bbcan.2020.188419
3. Jensen L, Guo Z, Sun X, Jing X, Yang Y, Cao Y. Angiogenesis, signaling pathways, and animal models. Chin Med J (Engl). 2025 May 20;138(10):1153-1162. DOI: 10.1097/CM9.0000000000003561
4. Shibuya M. Vascular Endothelial Growth Factor (VEGF) and Its Receptor (VEGFR) Signaling in Angiogenesis: A Crucial Target for Anti- and Pro-Angiogenic Therapies. Genes Cancer. 2011 Dec;2(12):1097-105. DOI: 10.1177/1947601911423031
5. Yao SX, Huang YJ, Zhang YX, Cui ZX, Lu HY, Wang R, Shi L. Revisiting VEGF/VEGFR-2 signalling as an anticancer target and its inhibitor discovery: where are we and where should we go?. Journal of drug targeting. 2025 Oct 21;33(9):1471-94.DOI: 10.1080/1061186X.2025.2508985
6. Scannevin RH, Alexander R, Haarlander TM, Burke SL, Singer M, Huo C, Zhang YM, Maguire D, Spurlino J, Deckman I, Carroll KI. Discovery of a highly selective chemical inhibitor of matrix metalloproteinase-9 (MMP-9) that allosterically inhibits zymogen activation. Journal of Biological Chemistry. 2017 Oct 27;292(43):17963-74. DOI: 10.1074/jbc.M117.806075
7. Folkman J. Tumor angiogenesis: therapeutic implications. New England Journal of Medicine. 1971;285(21):1182-1186. DOI: 10.1056/NEJM197111182852108
8. Kerbel RS. Tumor angiogenesis. New England Journal of Medicine. 2008;358(19):2039-2049. DOI:10.1056/NEJMra0706596
9. Ferrara N, Gerber HP, LeCouter J. The biology of VEGF and its receptors. Nature Medicine. 2003;9(6):669-676. DOI: 10.1038/nm0603-669
10. Hanahan D, Folkman J. Patterns and emerging mechanisms of the angiogenic switch during tumorigenesis. Cell. 1996;86(3):353-364. DOI: 10.1016/S0092-8674(00)80108-7
11. Jain RK. Normalization of tumor vasculature: an emerging concept in antiangiogenic therapy. Science. 2005;307(5706):58-62. DOI: 10.1126/science.1104819
12. Ellis LM, Hicklin DJ. VEGF-targeted therapy: mechanisms of anti-tumour activity. Nature reviews cancer. 2008 Aug;8(8):579-91. DOI: 10.1038/nrc2403
13. Hurwitz H, Fehrenbacher L, Novotny W, Cartwright T, Hainsworth J, Heim W, Berlin J, Baron A, Griffing S, Holmgren E, Ferrara N. Bevacizumab plus irinotecan, fluorouracil, and leucovorin for metastatic colorectal cancer. New England journal of medicine. 2004 Jun 3;350(23):2335-42. DOI: 10.1056/NEJMoa032691
14. Eremina V, Jefferson JA, Kowalewska J, Hochster H, Haas M, Weisstuch J, Richardson C, Kopp JB, Kabir MG, Backx PH, Gerber HP. VEGF inhibition and renal thrombotic microangiopathy. New England Journal of Medicine. 2008 Mar 13;358(11):1129-36. DOI: 10.1056/NEJMoa0707330
15. Chaudhari PJ, Nemade AR, Shirkhedkar AA. Recent updates on potential of VEGFR-2 small-molecule inhibitors as anticancer agents. RSC Adv. 2024 Oct 22;14(45):33384-33417. DOI: 10.1039/d4ra05244g
16. Elkaeed EB, Taghour MS, Mahdy HA, Eldehna WM, El-Deeb NM, Kenawy AM, A Alsfouk B, Dahab MA, Metwaly AM, Eissa IH, El-Zahabi MA. New quinoline and isatin derivatives as apoptotic VEGFR-2 inhibitors: design, synthesis, anti-proliferative activity, docking, ADMET, toxicity, and MD simulation studies. J Enzyme Inhib Med Chem. 2022 Dec;37(1):2191-2205. DOI: 10.1080/14756366.2022.2110869
17. Hussein NR, Sahib HB, Omran ZS (2026) The anti-angiogenic and anti-proliferative activity of n-benzoyl-3-phenyl isoserine derivative containing 1,2,3-triazole and quinoline rings. PLOS

ONE 21(5): e0344390. DOI: 10.1371/journal.pone.0344390

18. Li X, Wu C, Lin X, Cai X, Liu L, Luo G, You Q, Xiang H. Synthesis and biological evaluation of 3-aryl-quinolin derivatives as anti-breast cancer agents targeting ERα and VEGFR-2. European Journal of Medicinal Chemistry. 2019 Jan 1;161:445-55. DOI: 10.1016/j.ejmech.2018.10.045
19. Taghour MS, Elkady H, Eldehna WM, El-Deeb NM, Kenawy AM, Elkaeed EB, Alsfouk AA, Alesawy MS, Metwaly AM, Eissa IH. Design and synthesis of thiazolidine-2, 4-diones hybrids with 1, 2-dihydroquinolones and 2-oxindoles as potential VEGFR-2 inhibitors: In-vitro anticancer evaluation and in-silico studies. Journal of Enzyme Inhibition and Medicinal Chemistry. 2022 Dec 31;37(1):1903-17. DOI: 10.1080/14756366.2022.2085693
20. As T, Sal S. Synthesis and characterisation of substituted quinoline by Vilsmeier-Haack reagent. International Journal of Chemical Studies. 2017;5:1-4.
21. Nasab NH, Azimian F, Kruger HG, Kim SJ. Coumarin-chalcones generated from 3-Acetylcoumarin as a promising agent: synthesis and pharmacological properties. ChemistrySelect. 2022 Mar 22;7(11):e202200238. DOI: 10.1002/slct.202200238
22. Parquet E, Lin Q. Microwave assisted Wolff-Kishner reduction reaction. Journal of chemical education. 1997 Oct;74(10):1225.
23. McTigue M, Murray BW, Chen JH, Deng YL, Solowiej J, Kania RS. Molecular conformations, interactions, and properties associated with drug efficiency and clinical performance among VEGFR TK inhibitors. Proceedings of the National Academy of Sciences. 2012 Nov 6;109(45):18281-9. DOI: 10.1073/pnas.1207759109
24. Abdel-Kariem SM, Ali TE, Assiri MA, Shati AA, Alfaifi MY, Elbehairi SE. Novel chromone-based thiazolidinone-5-ylidene through hydrazone linker: synthesis, antiproliferative activity, apoptosis induction, cell cycle arrest, autophagy, in silico ADMET and molecular docking studies. Phosphorus, Sulfur, and Silicon and the Related Elements. 2025 Dec 2;200(12):985-1001. DOI: 10.1080/10426507.2025.2560493
25. Floch N, Finlay MR, Bianco A, Bickerton S, Colclough N, Cross DA, Cuomo EM, Guerot CM, Hargreaves D, Martin MJ, McKerrecher D. Evaluation of the therapeutic potential of phosphine oxide pyrazole inhibitors in tumors harboring EGFR C797S mutation. Cancer research. 2019 Jul 1;79(13_Supplement):4451. DOI: 10.1158/1538-7445.AM2019-4451
26. Alanzi AR, Moussa AY, Alsalhi MS, Nawaz T, Ali I. Integration of pharmacophore-based virtual screening, molecular docking, ADMET analysis, and MD simulation for targeting EGFR: A comprehensive drug discovery study using commercial databases. PLoS One. 2024 Dec 9;19(12):e0311527. DOI: 10.1371/journal.pone.0311527
27. Nuti E, Cuffaro D, D'Andrea F, Rosalia L, Tepshi L, Fabbi M, Carbotti G, Ferrini S, Santamaria S, Camodeca C, Ciccone L. Sugar-Based Arylsulfonamide Carboxylates as selective and water-soluble matrix metalloproteinase-12 inhibitors. ChemMedChem. 2016 Aug 5;11(15):1626-37. DOI: 10.1002/cmdc.201600235
28. Sanapalli BK, Yele V, Jupudi S, Karri VV. Ligand-based pharmacophore modeling and molecular dynamic simulation approaches to identify putative MMP-9 inhibitors. RSC advances. 2021 Aug 6;11(43):26820-31. DOI: 10.1039/d1ra03891e
29. Hattiholi A, Tendulkar S, Kumbar V, Rao M, Kugaji M, Muddapur U, Bhat K. Evaluation of anti-cancer activities of cranberries juice concentrate in osteosarcoma cell lines (MG-63). Indian Journal of Pharmaceutical Education and Research. 2022 Sep 23;56(4):1141-9. DOI: 10.5530/ijper.56.4.195
30. Peña-Morán OA, Villarreal ML, Álvarez-Berber L, Meneses-Acosta A, Rodríguez-López V. Cytotoxicity, post-treatment recovery, and selectivity analysis of naturally occurring podophyllotoxins from Bursera fagaroides var. fagaroides on breast cancer cell lines. Molecules. 2016 Aug 4;21(8):1013. DOI: 10.3390/molecules21081013
31. Souza-Tarla CD, Uzuelli JA, Machado AA, Gerlach RF, Tanus-Santos JE. Methodological issues affecting the determination of plasma matrix metalloproteinase (MMP)-2 and MMP-9 activities. Clinical biochemistry. 2005 May 1;38(5):410-4. DOI: 10.1016/j.clinbiochem.2005.02.010
32. Snoek-van Beurden PA, Von den Hoff JW. Zymographic techniques for the analysis of matrix metalloproteinases and their inhibitors. Biotechniques. 2005 Jan 1;38(1):73-83. DOI: 10.2144/05381RV01

33. Donald L. Pavia, Gary M. Lampman, George S. Kriz, and James R. Vyvyan. Introduction to Spactroscopy. 5th ed. Cengage; 2015.
34. Silverstein RM, Webster FX. Spectrometric Identification of Organic Compounds. 6th ed. Wiley, Newyok; 2003.
35. Skoog DA, Crouch SR, James HF. Principles of Instrumental Analysis. 6th ed. Cengage; 2016.
36. Puskullu MO, Celik I, Erol M, Fatullayev H, Uzunhisarcikli E, Kuyucuklu G. Antimicrobial and antiproliferative activity studies of some new quinoline-3-carbaldehyde hydrazone derivatives. Bioorganic Chemistry. 2020 Aug 1;101:104014. DOI: 10.1016/j.bioorg.2020.104014
37. Korcz M, Sączewski F, Bednarski PJ, Kornicka A. Synthesis, structure, chemical stability, and in vitro cytotoxic properties of novel quinoline-3-carbaldehyde hydrazones bearing a 1, 2, 4-triazole or benzotriazole moiety. Molecules. 2018 Jun 20;23(6):1497. DOI: 10.3390/molecules23061497